Journal of Experimental Nanoscience
Publication details, including instructions for authors and subscription information:
http://www.informaworld.com/smpp/title~content=t716100757

Fabrication of In-doped SnO_2 nanowire arrays and its field emission investigations

Ashok B. Bhise[a]; Dattatray J. Late[ab]; B. Sathe[c]; Mahendra A. More[a]; Imtiaz S. Mulla[c]; Vijayamohanan K. Pillai[c]; Dilip S. Joag[a]
[a] Center for Advanced Studies in Material Science and Condensed Matter Physics, Department of Physics, University of Pune, Pune 411007, India [b] Jawaharlal Nehru Centre for Advanced Scientific Research, Bangalore 560064, India [c] Physical and Materials Chemistry Division, National Chemical Laboratory, Pune 411008, India

Online publication date: 17 December 2010

To cite this Article Bhise, Ashok B. , Late, Dattatray J. , Sathe, B. , More, Mahendra A. , Mulla, Imtiaz S. , Pillai, Vijayamohanan K. and Joag, Dilip S.(2010) 'Fabrication of In-doped SnO_2 nanowire arrays and its field emission investigations', Journal of Experimental Nanoscience, 5: 6, 527 — 535
To link to this Article: DOI: 10.1080/17458081003671683
URL: http://dx.doi.org/10.1080/17458081003671683

Journal of Experimental Nanoscience
Vol. 5, No. 6, December 2010, 527–535

Taylor & Francis
Taylor & Francis Group

Fabrication of In-doped SnO_2 nanowire arrays and its field emission investigations

Ashok B. Bhise[a], Dattatray J. Late[ab], B. Sathe[c], Mahendra A. More[a], Imtiaz S. Mulla[c], Vijayamohanan K. Pillai[c] and Dilip S. Joag[a]*

[a]*Center for Advanced Studies in Material Science and Condensed Matter Physics, Department of Physics, University of Pune, Pune 411007, India;* [b]*Jawaharlal Nehru Centre for Advanced Scientific Research, Jakkur P.O., Bangalore 560064, India;* [c]*Physical and Materials Chemistry Division, National Chemical Laboratory, Pune 411008, India*

(*Received 28 January 2009; final version received 2 February 2010*)

The field emission of In-doped SnO_2 wire array has been performed in parallel plate diode configuration. A maximum current density of $60\,\mu A/cm^2$ is drawn from the emitter at an applied field of $4\,V/\mu m$. The nonlinearity in the Fowler–Nordheim plot, characteristics of semiconductor emitter has been observed and explained on the basis of electron emission from both the conduction and the valence bands. The current stability recorded at a preset value of $1\,\mu A$ is observed to be good. The high emission current density, good current stability and mechanically robust nature of the wires offer unprecedented advantages as promising cold cathodes for many potential applications based on field emission.

Keywords: field emission; doping; SnO_2; nanowires; cold cathodes; device

1. Introduction

Various nanostructure materials such as nanotubes, nanowires, nanobelts and nanorods of various materials such as CNTs [1], ZnO [2,3], SnO_2 [4], In_2O_3 [5], Si [6], SiC [7], Cu_2S [8], etc., exhibit excellent field emission properties due to the high aspect ratio. Tin oxide, as n-type and wide band gap ($E_g = 3.6\,eV$) [9] semiconductor nanostructure, has potential for the applications in various field emission-based devices. It has been intensively investigated due to its inherent properties and anticipated applications in many areas such as chemical and gas sensors [10], solar cells, transistors, conducting electrodes and optoelectronic devices [9,11]. One-dimensional tin oxide nanostructures, due to their ability to introduce foreign atoms into the crystal lattice to specifically tailor the electrical and optical properties, make them highly versatile [11]. To reduce their resistivity with much higher carrier concentration and mobility, SnO_2 nanostructures are doped with various metals and metal oxides [12,13]. Furthermore, the n-type doping is known to enhance field emission by lifting the fermi level and lowering the work function. The

*Corresponding author. Email: dsj@physics.unipune.ernt.in

ISSN 1745–8080 print/ISSN 1745–8099 online

DOI: 10.1080/17458081003671683
http://www.informaworld.com

indium-doped tin oxide (ITO), an important transparent metal-oxide semiconductor, with the advantage of lower surface potential barrier than that of the metals, has been widely investigated [14–18].

The field emitter arrays have an ability to pack a large number of identical emitters into small areas and precision with which an individual emitter may be positioned. Since the current generated from a single microtip is quite small, arrays are suitable for the application in areas where very high current densities are required such as vacuum micro/nanoelectronic devices, flat panel displays, large area electronics and cold cathode electron sources. Here, we report on the synthesis of In–SnO_2 wires on Au-patterned silicon substrates by thermal evaporation and its field electron emission properties.

2. Experimental technique

In order to obtain the position controlled and patterned growth of In–SnO_2 nanowires, gold (Au) with a film of thickness ~10 nm was deposited on the clean silicon (1 0 0) substrates using vacuum deposition and patterned photolithographically into micro-patterned square arrays, $400 \times 400\,\mu m^2$, so as to grow indium-doped tin oxide nanowires (In–SnO_2), on Au-patterned Si substrates. Thoroughly mixed In and SnO powders in the weight ratio 0.8–1.2mg:50 mg were loaded in the alumina boat as a source material. The In and SnO powder were 99.99% pure and were purchased from Sigma–Aldrich (USA). The patterned Si substrates were placed in the alumina boat with the patterned side upside down facing the source. The alumina boat was carefully positioned at the centre of the horizontal tube furnace. Then, the furnace was rapidly heated to 950°C at the rate of 3°C/min. The argon gas was continuously passed at a flow rate of 100 sccm. The growth lasted for 3 h in argon atmosphere. After cooling the furnace down to room temperature without interrupting the Ar gas a flow, a whitish–grey reaction product containing nanowires was found to grow on the Au-patterned side of the Si substrate.

The crystal structure of the as-deposited nanowires on Si substrate was characterised by X-ray Diffraction (XRD) spectrometer (Model-D8 Advance, Bruker AXS). The surface morphology of the as-synthesised product was examined by scanning electron microscopy (SEM) (Model-JEOL, JSM-6360). The chemical composition of the as-deposited In–SnO_2 wire product on silicon substrate was analysed by energy dispersive X-ray analysis (EDAX) attached to SEM. In order to investigate the field emission properties of the as-synthesised In–SnO_2 nanowires, the silicon substrate with the as-deposited In–SnO_2 nanowires was stuck to the stainless steel stub attached to the linear motion drive with vacuum compatible silver paste which served as the emitter cathode. The tin oxide-coated conducting glass, deposited with fluorescent powder, served as an anode screen. The emitter cathode was mounted in parallel and in front of the anode screen, facing the phosphor-coated side, at a distance of 1 mm. The emission sites could be seen directly on the screen. This parallel plate diode assembly comprising emitter cathode and anode screen was mounted on an all metal ultra high vacuum (UHV) system for evacuation. The UHV system comprises a turbomolecular pump, a sputter ion pump and a titanium sublimation pump with a liquid nitrogen trap. After baking the system for 10 h at 250°C, a pressure better than 1×10^{-9} mbar was routinely achieved in the system and maintained by the sputter ion pump. The field emission current–voltage measurements were carried out in parallel plate diode configuration at various values of cathode–anode separation.

The current–voltage (I–V) and current–time (I–t) stability measurements were carried at this base pressure using Spellman high voltage power supply and a Keithley 485 picoammeter. Special care has been taken to avoid current leakage. The field emission experiments were repeated at least on three different specimens synthesised under identical experimental conditions to check the reproducibility of the results.

3. Results and discussion

Figure 1 shows the XRD pattern of the as-synthesised In–SnO_2 wires on Au-patterned silicon substrate. All the diffraction peaks are indexed to the tetragonal rutile structure of SnO_2, which agree well with the reported values ($a = 4.738$ Å and $c = 3.187$ Å) from JCPDS card (21-1250). In-doped SnO_2 nanowires show some strain in the system which is manifested in distortion and minimal shift in XRD peak positions when compared to the pure tin oxide. Moreover, slight distortions to the parent tetragonal rutile structure have been reported in the literature for higher doping percentages of indium. Figure 2 shows EDAX spectrum of the as-deposited In–SnO_2 wires. The EDAX analysis indicates that the elemental composition of indium in the In–SnO_2 nanowire is 4–5 at. wt% of In in SnO_2 molecular weight. The evaporation temperature of indium is approximately 600°C and the same for tin oxide is quite high. Now the presence of one component in the evaporation boat can influence the evaporation temperature of another. For example, the presence of indium here can cause slight reduction in evaporation temperature. Moreover, if the maximum temperature used in the experiment (950°C) is larger than the evaporation temperature of both the components, then the rate of evaporation of the component having lower evaporation temperature will be higher due to the latent heat required for the phase transformation. Therefore, the final composition of the nanowire material (here In-doped tin oxide) will be different as compared to that of the precursor material components.

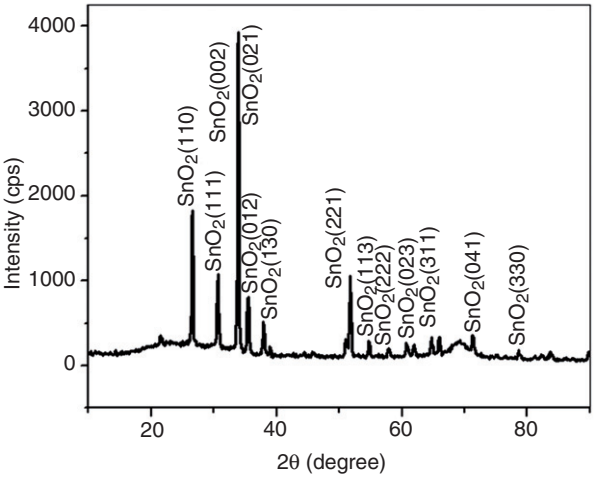

Figure 1. XRD pattern of the as-synthesised patterned arrays of In–SnO_2 on Si substrates.

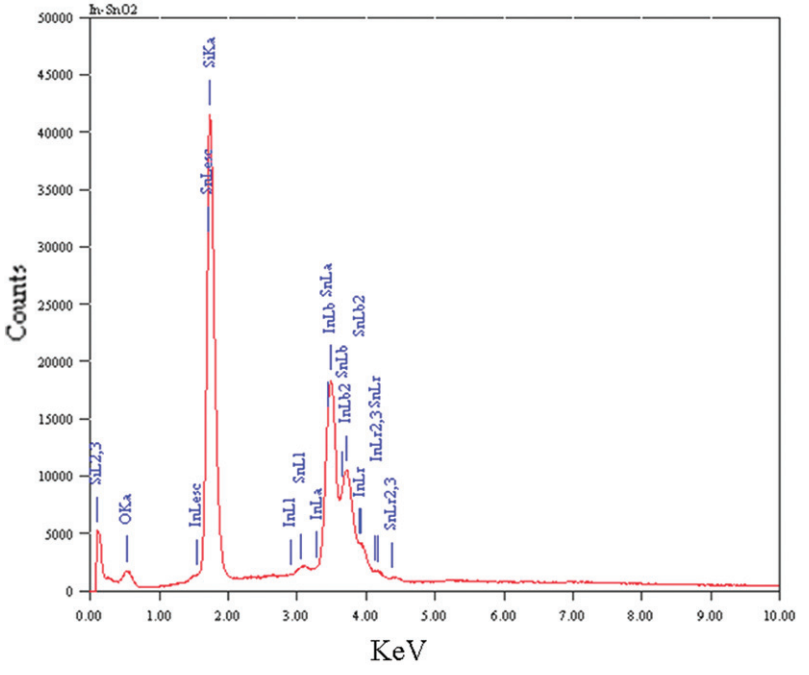

Figure 2. EDAX spectrum of the synthesised patterned arrays of In–SnO_2.

Therefore, less atomic weight percentage of indium was taken in our experiment. Considering the larger rate of deposition of indium, several wt% of indium were tried with 50 mg of tin oxide and it was found that 0.8–1.2 mg of In into 50 mg of tin oxide results in 4–5 at.% of In into the tin oxide system.

Figure 3(a) depicts the SEM image of the photolithograpically patterned arrays of In–SnO_2 and Figure 3(b)–(d) shows a high magnification SEM images of In–SnO_2 nanowire arrays. The high areal density wires were easily grown on Au electrodes deposited on silicon substrates, leaving the bare silicon surface with little wires. The wires were randomly grown on Au electrodes patterned on silicon substrates.

Figure 4 shows the field emission *I–V* curves at various values of cathode–anode separation. The turn on field, defined as the field required at a current density of 1 $\mu A/cm^2$, was 1.28 V/μm at $d = 2$ mm. From the *I–V* measurements, the Fowler–Nordheim (F–N) [19,20] plots were drawn. Figure 5 shows the corresponding F–N plots of the In–SnO_2 wire arrays at various values of cathode–anode distance '*d*'. The nature of F–N plots indicates that the electron emission process from In–SnO_2 wires is a quantum mechanical barrier tunnelling phenomenon. An interesting nonlinear behaviour of the F–N plot is observed, which could be clearly understood for two ranges of the applied field, low and high. Such a nonlinear behaviour of the F–N plot, typical for a semiconductor emitter, has been observed previously for semiconductor emitter [21–25], which has been attributed to the origin of field-emitted electrons. In the low-field region, the emission current is due to the conduction band electrons, whereas in the high-field region, electrons from both

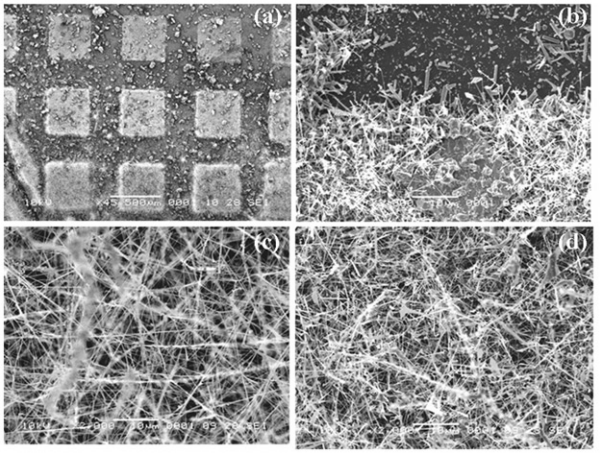

Figure 3. SEM images of the (a) as-synthesised photolithographic pattern, (b) In–SnO_2 nanowires deposited on Si photolithographic pattern substrates and (c and d) high magnification SEM images of In–SnO_2 nanowires.

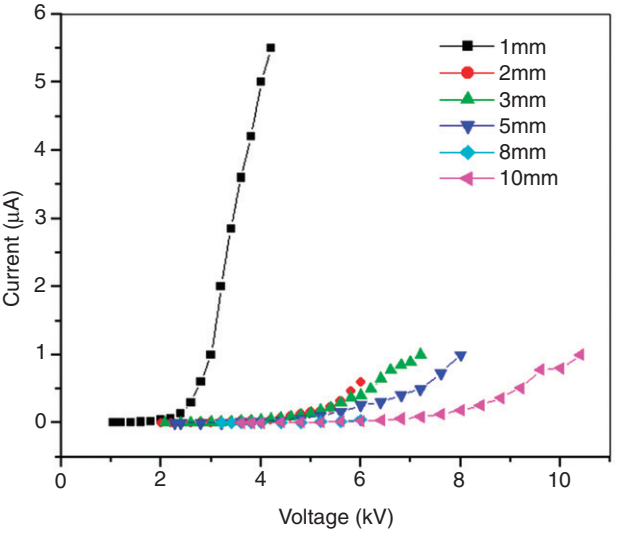

Figure 4. Field emission current–voltages (I–V) characteristics at various cathode–anode separation distances.

the conduction and the valence bands contribute to the observed field emission current. From the slope of the F–N plot, using the formula for the field enhancement factor (β) [19,20]

$$\beta = -6.8 \times 103 \times \frac{\phi^{3/2}}{m},$$

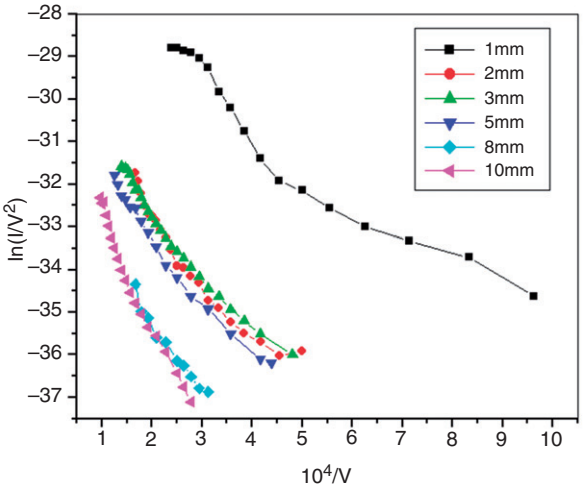

Figure 5. F–N plot corresponding to *I–V* at various separation distances.

where m is the slope of F–N plot in low-field region and φ the work function of In–SnO_2 wire (adopting $\varphi = 4.3$ eV in this case [21]); β was estimated to be 29,229 cm^{-1} at $d = 2$ mm. This high value of β indicates that the electron emission is from nanometric dimensions of the emitters. Earlier such values of field enhancement factor were reported by Wan et al. [26] and Zhao et al. [27] for arrays of SnO_2 wires.

It is well known that the densities of Sn and In are almost the same in contrast to Fe and Ru. Moreover, the melting points of In and Sn are close (156.5 and 231°C, respectively) while these values for Fe and Ru are very large (1535 and 2330°C, respectively). Due to this compatibility of Sn and In, it is easy for In to be doped in Sn matrix, while other metals Fe and Ru, will not have efficient doping into Sn matrix. When In is doped into SnO_2 system it yields low threshold field emission and high emission current density along with the good emission stability as a result of more nanometric dimension of nanowires. These characteristics are not achieved for Fe and Ru doping into SnO_2 system. The In-doped SnO_2 system shows enhanced field emission characteristics due to the finer SnO_2 nanowire dimensions and hence a higher aspect ratio. The field enhancement factor in the present case is higher as compared to the earlier reported values for Fe-doped SnO_2 and Ru-doped SnO_2 systems due to the sharp features of the nanowires [21–25].

The current density (J) defined as the ratio of the maximum current drawn to the area covered by Au electrodes on the silicon substrates, calculated using $J = I/A$, comes out to be 60 $\mu A/cm^2$, where I is the emission current and A is the substrate dimension (5×5 mm^2). A current density as high as 60 $\mu A/cm^2$ at a field of 4 V/μm was drawn. This value of current density is comparable to that of ZnO nanowire arrays [2] and carbon nanotube arrays [16] and higher than that of patterned SnO_2 nanostructures [4]. The large current density may be attributed to the high aspect ratio and improved electrical conductivity of the In–SnO_2 wires.

The field emission current stability was recorded at the preset current value of 1 μA over a 3 h duration of measurement at $d = 2$ mm. We have carried out a current–time

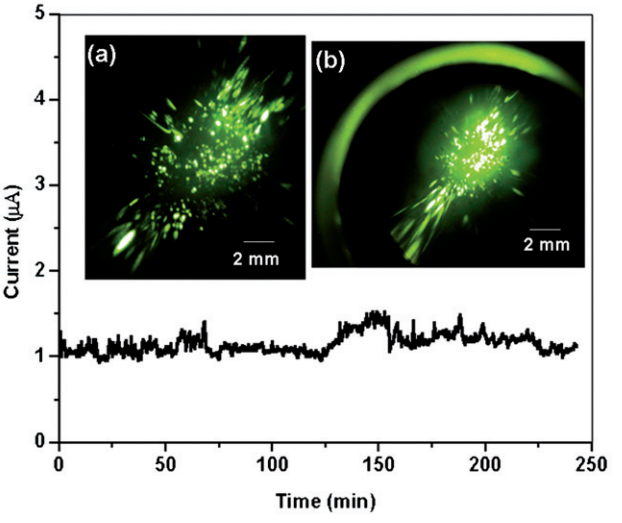

Figure 6. Current–time (*I–t*) plot for patterned arrays of In–SnO_2 on Si substrates. The inset shows the corresponding field emission image recorded at (a) 4 kV and (b) 6 kV.

measurement experiment at $\sim 1 \times 10^{-9}$ mbar vacuum, where H_2 and CO are mainly present. The *I–t* curve is as shown in Figure 5, which depicts that the field emission current from In–SnO_2 wire arrays is stable over the period (3 h) of measurements. The fluctuations in the field emission current were calculated by dividing the maximum fluctuation by average current and are observed to be less than 5%. The high stability of the emission current is due to the oxidation resistant behaviour of In–SnO_2 wires. The small fluctuations in the emission current are due to the adsorption and desorption of residual gas molecules at the emitter surfaces. The inset of Figure 6 shows the field emission images recorded at two different voltages: (a) 4 kV and (b) 8 kV. The images obtained are stable and intense. The post-field emission SEM observation shows no significant change in the emitter surface morphology of the In–SnO_2 wire arrays indicating the excellent mechanical stability.

4. Conclusion

In conclusion, the high current density 60 μA/cm^2 at the applied electric field of 4 V/μm has been obtained from In–SnO_2 arrays. The high value field enhancement factor 29,229 cm^{-1} indicated the electron emission from nanometric dimension of the emitters. The good current stability indicated that the In–SnO_2 wire arrays were the potential candidate for field emission-based new generation devices.

References

[1] O.J. Lee, S.H. Jeong, and K.H. Lee, *Fabrication of field emitter arrays of carbon nanotubes aligned on patterned substrates using self-assembly monolayer*, Mater. Res. Soc. Proc. 772 (2003), pp. M7.7.

[2] E.C. Greyson, Y. Babayan, and T.W. Odom, *Directed growth of ordered arrays of small diameter ZnO nanowires*, Adv. Mater. 16 (2004), pp. 1348–1352.
[3] D.J. Late, P. Misra, B.N. Singh, L.M. Kukreja, D.S. Joag, and M.A. More, *Enhanced field emission from pulsed laser deposited nanocrystalline ZnO thin films on Re and W*, Appl. Phys. A: Mater. Sci. Process. 95 (2009), pp. 613–620.
[4] Y.J. Chen, Q.H. Li, Y.X. Liang, T.H. Wang, Q. Zhao, and D.P. Yu, *Field emission from long SnO_2 nanobelt arrays*, Appl. Phys. Lett. 85 (2004), pp. 5682–5684.
[5] S. Kar, S. Chakrabarti, and S. Chaudhuri, *Morphology dependent field emission from In_2O_3 nanostructures*, Nanotechnology 17 (2006), pp. 3058–3062.
[6] Y.M. Fung, W.Y. Cheung, I.H. Wilson, J.B. Xu and S.P. Wong, *Silicon field emitter array by fast anodization method*, Mater. Res. Soc. Symp. Proc. 621 (2000), pp. R.5.4.
[7] Z.W. Pan, H.L. Iai, F.C.K. Au, X.F. Duan, W.Y. Zhou, W.S. Shi, N. Wang, C.S. Lee, N.B. Wong, S.T. Lee, and S.S. Xie, *Oriented silicon carbide nanowires: Synthesis and field emission properties*, Adv. Mater. 12 (2000), pp. 1186–1190.
[8] J. Chen, S.Z. Deng, N.S. Xu, S. Wang, X. Wen, S. Yang, C. Yang, and W. Ge, *Field emission from crystalline copper sulphide nanowire arrays*, Appl. Phys. Lett. 80 (2002), pp. 3620–3622.
[9] E.R. Leite, I.T. Weber, E. Longo, and J.A. Varela, *A new method to control particle size and particle size distribution of SnO_2 nanoparticles for gas sensor applications*, Adv. Mater. 12 (2000), pp. 965–968.
[10] Y. Zhang, K. Yu, L. Guodong, D. Peng, Q. Zhang, F. Xu, W. Bai, S. Ouyang, and Z. Zhu, *Synthesis and field emission of patterned SnO_2 nanoflowers*, Mater. Lett. 60 (2006), pp. 3109–3112.
[11] B.Y. Wei, M.C. Hsu, P.G. Su, H.M. Lin, R. Jang, and H.J. Lai, *A novel SnO_2 gas sensor doped with carbon nanotubes operating at room temperature*, Sens. Actuators B 101 (2004), pp. 81–89.
[12] P. Nguyen, H.T. Ng, J. Kong, A.M. Cassell, R. Quinn, J. Li, J. Han, M. McNeil, and M. Meyyappan, *Epitaxial directional growth of indium-doped tin oxide nanowire arrays*, Nano Lett. 3 (2003), pp. 925–929.
[13] H. Kim and A. Pique, *Transparent conducting Sb-doped SnO_2 thin films grown by pulsed-laser deposition*, Appl. Phys. Lett. 84 (2004), pp. 218–220.
[14] I.M. Chan, T.Y. Hus, and F.C. Hong, *Enhanced hole injections in organic light-emitting devices by depositing nickel oxide on indium tin oxide anode*, Appl. Phys. Lett. 81 (2002), pp. 1899–1901.
[15] C.W. Tang and S.A. Van Slyke, *Organic electroluminescent diodes*, Appl. Phys. Lett. 51 (1987), pp. 913–915.
[16] Q. Wan, K. Yu, T.H. Wang, and C.L. Lin, *Low-field electron emission from tetrapod-like ZnO nanostructures synthesized by rapid evaporation*, Appl. Phys. Lett. 83 (2003), pp. 2253–2255.
[17] J.M. Bonard, K.A. Dean, B.F. Coil, and C. Klinke, *Field emission of individual carbon nanotubes in the scanning electron microscope*, Phys. Rev. Lett. 89 (2002), pp. 197602–197605.
[18] Y. Zhang, K. Yu, G. Li, D. Peng, Q. Zhang, H. Hu, F. Xu, W. Bai, S. Ouyang, and Z. Zhu, *Field emission from patterned SnO_2 nanostructures*, Appl. Surf. Sci. 253 (2006), pp. 792–796.
[19] R.H. Fowler and L.W. Nordheim, *Electron emission in intense electric field*, Proc. R. Soc. London, Ser. A 119 (1928), pp. 173–200, (doi: 10.1098/rspa.1928.0091).
[20] R. Gomer, *Field Emission and Field Ionization*, American Vacuum Society Classics, Woodbury/AIP, New York, 1993.
[21] A.B. Bhise, D.J. Late, P. Walke, M.A. More, I.S. Mulla, V.K. Pillai, and D.S. Joag, *A single In-doped SnO_2 submicrometre sized wire as a field emitter*, J. Phys. D: Appl. Phys. 40 (2007), pp. 3644–3648.
[22] A.B. Bhise, D.J. Late, P.S. Walke, M.A. More, V.K. Pillai, I.S. Mulla, and D.S. Joag, *Sb-doped SnO_2 wire: Highly stable field emitter*, J. Crys. Growth 307 (2007), pp. 87–91.
[23] A.B. Bhise, D.J. Late, N.S. Ramgir, M.A. More, I.S. Mulla, V.K. Pillai, and D.S. Joag, *Field emission investigations of RuO_2-doped SnO_2 wires*, Appl. Surf. Sci. 253 (2007), pp. 9159–9163.

[24] A.B. Bhise, D.J. Late, N.S. Ramgir, M.A. More, I.S. Mulla, V.K. Pillai, and D.S. Joag, *RuO_2 doped SnO_2 nanobipyramids on Si (100) as a field emitter*, Thin Solid Films 516 (2008), pp. 6388–6391.
[25] A.B. Bhise, D.J. Late, B.R Sathe, M.A. More, I.S. Mulla, V.K. Pillai, and D.S. Joag, *Field emission investigation of single Fe-doped SnO_2 wire*, Solid State Sci. 11 (2009), pp. 1114–1117.
[26] Q. Wan, P. Feng, and T.H. Wang, *Vertically aligned tin-doped indium oxide nanowire arrays: Epitaxial growth and electron field emission properties*, Appl. Phys. Lett. 89 (2006), pp. 123102–123105.
[27] Q. Zhao, H.Z. Zhang, Y.W. Zhu, S.Q. Feng, X.C. Sun, J. Xu, and D.P. Yu, *Morphological effects on the field emission of ZnO nanorod arrays*, Appl. Phys. Lett. 86 (2005), pp. 203115–203117.